Proc. Natl. Acad. Sci. USA
Vol. 92, pp. 8115–8119, August 1995
Cell Biology

Direct evidence for tumor necrosis factor-induced mitochondrial reactive oxygen intermediates and their involvement in cytotoxicity

VERA GOOSSENS, JOHAN GROOTEN, KURT DE VOS, AND WALTER FIERS*

Laboratory of Molecular Biology, Ghent University, K.L. Ledeganckstraat 35, B-9000 Ghent, Belgium

Communicated by Marc Van Montagu, Ghent University, Ghent, Belgium, May 19, 1995

ABSTRACT **Tumor necrosis factor (TNF) is selectively cytotoxic to some types of tumor cells *in vitro* and exerts antitumor activity *in vivo*. Reactive oxygen intermediates (ROIs) have been implicated in the direct cytotoxic activity of TNF. By using confocal microscopy, flow cytometry, and the ROI-specific probe dihydrorhodamine 123, we directly demonstrate that intracellular ROIs are formed after TNF stimulation. These ROIs are observed exclusively under conditions where cells are sensitive to the cytotoxic activity of TNF, suggesting a direct link between both phenomena. ROI scavengers, such as butylated hydroxyanisole, effectively blocked the formation of free radicals and arrested the cytotoxic response, confirming that the observed ROIs are cytocidal. The mitochondrial glutathione system scavenges the major part of the produced ROIs, an activity that could be blocked by diethyl maleate; under these conditions, TNF-induced ROIs detectable by dihydrorhodamine 123 oxidation were 5- to 20-fold higher.**

The pleiotropic cytokine tumor necrosis factor (TNF), primarily produced by activated macrophages, exerts a wide range of inflammatory and immunomodulatory activities—for example, as a crucial mediator in septic shock and as an activator of human immunodeficiency virus replication. In addition, TNF, especially in combination with interferon γ, selectively kills a variety of tumor cell lines *in vitro* and has antitumor activity *in vivo* (1, 2). The molecular basis of the selective cytotoxic action against tumor cells is still not fully understood. Studies, mainly based on specific inhibitors, have indicated that multiple intracellular pathways may be involved in TNF signaling, depending on the cell type. Among the reported effects are G-protein-coupled activation of phospholipases (3), extracellular release of arachidonic acid (3), formation of reactive oxygen intermediates (ROIs) (4–6), and activation of protein kinases and proteases (7, 8) and sphingomyelinases (9).

ROIs are involved in many biological processes. Increased levels of free radicals take part in the defence against microorganisms (10), act as secondary messengers for activation of the transcription factor NF-κB, or directly cause cell injury, for example, by lipid peroxidation (11). Evidence obtained so far for a role of ROIs in TNF-mediated cytotoxicity was mostly indirect. The protective effect exerted by overexpressed manganese superoxide dismutase, radical scavengers, iron chelators, and inhibitors or elimination of the mitochondrial electron transport chain in appropriate cell lines (6, 12, 13) provide substantial evidence for the involvement of ROIs in TNF-mediated cytotoxicity and point to the mitochondria as the probable source of ROIs. However, the exact nature of the role played by ROIs in TNF signaling—namely, as secondary messengers and/or as direct mediators of cytotoxicity—is still not established and is the topic of this report.

The publication costs of this article were defrayed in part by page charge payment. This article must therefore be hereby marked "*advertisement*" in accordance with 18 U.S.C. §1734 solely to indicate this fact.

To determine the mechanism by which mitochondria contribute to cytotoxicity, we analyzed the levels of intracellular ROI formation in individual TNF-treated L929 cells, by using a cell-permeable ROI-specific fluorogenic marker, dihydrorhodamine 123 (DHR123) (14, 15). ROI-generated fluorescence was analyzed on individual cells by confocal laser scanning microscopy (CLSM) and by flow cytometry and was linked to the progression of cytotoxic response. The results demonstrate that (*i*) free radicals are induced shortly before the occurrence of irreversible cell damage; (*ii*) TNF-mediated ROI formation is strictly correlated with cytotoxicity and represents an essential step in the cytotoxic process; and (*iii*) TNF-induced ROIs are presumably produced in the mitochondria, as a result of interference with the normal electron flow, and are largely scavenged by the mitochondrial glutathione (GSH) system.

MATERIALS AND METHODS

Cell Culture. L929, a murine fibrosarcoma cell line, and its TNF-resistant derivatives L929r1 and L929r2 (16) were grown in Dulbecco's modified Eagle's medium supplemented with 10% (vol/vol) heat-inactivated fetal calf serum, penicillin (100 units/ml), and streptomycin (0.1 mg/ml). All cell lines were mycoplasma-free, as judged by a DNA fluorochrome assay (17). Suspension cultures of adherent L929 cells were obtained by seeding cells, harvested from cultures in tissue culture flasks by trypsinization at 37°C, in 30- or 90-mm diameter bacterial-grade Petri dishes at $4 \times 4\ 10^5$ cells per ml in 3–6 ml of complete medium. Cultures were preincubated overnight at 37°C in a humidified 5% CO_2/95% air incubator prior to TNF treatment. Under these conditions, the cells no longer adhered to the plastic surface and remained in suspension. TNF sensitivity of the cells was not altered in these suspension cultures (18).

TNF and Reagents. Recombinant murine TNF was produced in *Escherichia coli* and purified to at least 99% homogeneity (19). The preparation had a specific activity of 1.2×10^8 international units (IU) per mg of protein and contained 4 ng of endotoxin per mg of protein. TNF activity was determined as described (20), by using an international standard TNF preparation (code no. 88/532; Institute for Biological Standards and Control, Potters Bar, U.K.) as a reference. Cycloheximide (CHX) was dissolved in culture medium and, where mentioned, was added to 50 μg/ml. Propidium iodide (PI; Becton Dickinson) was prepared as a 3 mM stock solution in phosphate-buffered saline and stored at 4°C. Where men-

Abbreviations: BCNU, 1,3-bis(2-chloroethyl)-1-nitrosourea; BHA, butylated hydroxyanisole; BHT, butylated hydroxytoluene; BSO, buthionine sulfoximine; CHX, cycloheximide; CLSM, confocal laser scanning microscopy; DEM, diethyl maleate; DHR123, dihydrorhodamine 123; FALS, forward-angle light scatter; GSH, glutathione; IL, interleukin; PI, propidium iodide; R123, rhodamine 123; ROIs, reactive oxygen intermediates; TNF, tumor necrosis factor; 90LS, 90°-angle light scatter; IU, international unit(s).

*To whom reprint requests should be addressed.

tioned, PI was added to 30 μM. The fluorescent marker DHR123 was purchased from Molecular Probes, prepared as a 5 mM stock solution in dimethyl sulfoxide, and used at 1 μM. Stock solutions of butylated hydroxyanisole (BHA) and butylated hydroxytoluene (BHT) were prepared in ethanol; buthionine sulfoximine (BSO) and diethyl maleate (DEM) were dissolved in culture medium. These chemicals were purchased from Sigma. 1,3-bis(2-Chloroethyl)-1-nitrosourea (BCNU) from Bristol-Myers Squibb was dissolved in dimethyl sulfoxide.

Measurement of ROI Formation by CLSM. Cells were seeded in coverslip chambers (Lab-Tek; Nunc) at 3×10^5 cells per chamber (2 cm^2) and TNF was added at 1000 IU/ml. At appropriate time points prior to or during TNF treatment, cells were loaded with DHR123 for at least 30 min at 37°C in a humidified 5% CO_2/95% air incubator. After loading, the marker was washed away by several medium changes and the cells were immediately observed on a Zeiss model LSM 410 invert on the basis of a Zeiss Axiovert 100 microscope. Rhodamine 123 (R123) derived from DHR123 by oxidation was excited with an argon ion laser at 488 nm. Fluorescent emission of the marker was detected between 515 and 565 nm. To determine cell death, PI was added to the culture chambers after DHR123 loading, 3–10 min before microscopic examination. Fluorescence emission by PI-positive cells was excited at 488 nm and detected above 610 nm. Images from individual samples were collected by using the same detector sensitivity and zoom factor. The kinetics of R123 and PI fluorescence in single cells was determined by a slight modification of the above protocol: cells were loaded with DHR123 for 30 min, TNF (1000 IU/ml) and PI were added, and a single microscopic field was observed for up to 7 hr while the coverslip chamber was maintained at 37°C by a heated microscopic stage.

Measurement of ROI Formation and Cell Death by Flow Cytometry. DHR123 was added to suspension cultures at the same time as TNF (1000 IU/ml). Cell samples were taken at regular time intervals and analyzed on an EPICS 753 flow cytometer (Coulter). R123 fluorescence resulting from DHR123 oxidation was excited with a water-cooled argon ion laser (250 mW) at 488 nm and detected between 515 and 550 nm. Cell death was calculated from the number of collapsed cells, detected as a distinct population exhibiting a reduced forward angle light scatter (FALS) in a two-parameter FALS × 90°-angle light scatter (90LS) histogram (18). R123 fluorescence (after DHR123 staining) was exclusively analyzed on cells exhibiting FALS × 90LS properties characteristic of viable cells. Three thousand viable cells were measured per sample. Cell debris and multicell aggregates were electronically gated out. The variation on both measurements was determined on independent samples and was consistently <10% for ROI and <8% for cell death.

Interleukin (IL) 6 Bioassay. The presence of IL-6 bioactivity in the culture supernatants of 4×10^5 cells, seeded in 24-well dishes, was determined 5–12 hr after addition of TNF, on the basis of the proliferative response of the mouse plasmacytoma cell line 7TD1 (21).

Measurement of Intracellular GSH. Cells were seeded in 96-microwell culture plates at 5×10^4 cells in 200 μl of medium. Monochlorobimane (22) was dissolved in dimethyl sulfoxide to 0.16 M and added to the cells to 400 μM. The cultures were further incubated for 45 min at 37°C, the medium was refreshed, and fluorescence was measured in a Cytofluor 2300 apparatus (Millipore) at 480 nm by using an excitation wavelength of 360 nm.

RESULTS

Detection of TNF-Induced ROI Formation by CLSM. DHR123 is a cell-permeable fluorogenic marker specific for ROIs, mainly H_2O_2 and possibly $O_2^{\cdot-}$. Oxidation of the nonfluorescent DHR123 by these radical species yields the cationic fluorescent R123, which is subsequently sequestered by active mitochondria (15). Hence, the accumulation of R123 fluorescence is used as a measure of ROI formation. The optical probe DHR123 was preferred over the frequently used dichlorofluorescein diacetate, because the latter probe is, unlike DHR123/R123, subject to leakage from the cell at 37°C. Transmitted light images (Fig. 1 *A* and *D*), confocal fluorescence images after DHR123 (green) and PI (red) staining (Fig. 1 *B* and *E*), and three-dimensional representa-

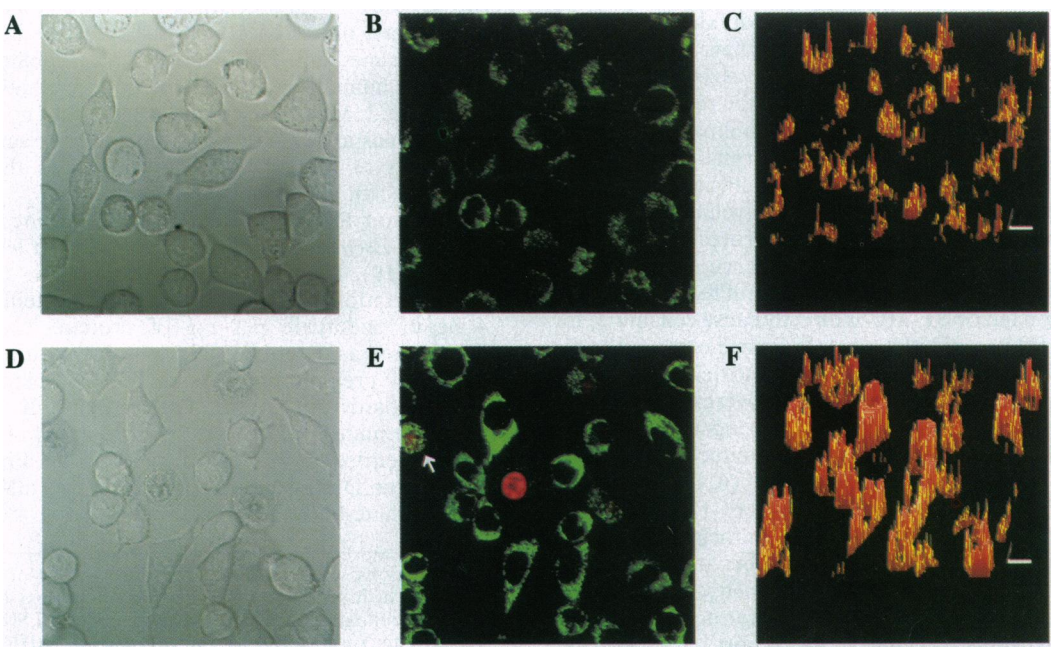

FIG. 1. Transmission images (*A* and *D*), CLSM fluorescence images (*B* and *E*), and three-dimensional representation of the fluorescence images (*C* and *F*) (the height matches the green fluorescence intensity observed in *B* and *E*). L929 cells were untreated (*A–C*) or treated (*D–F*) with TNF (1000 IU/ml) for 3 hr (the arrow points to a double-fluorescent cell). Cells were stained with DHR123 for 30 min at 37°C (green). PI was added to culture chambers shortly before microscopic examination (red). (Bars = angle of incidence.)

tions of the intensity of the accumulated R123 fluorescence distribution in individual cells (Fig. 1 *C* and *F*) are shown for untreated cells (Fig. 1 *A–C*) and TNF-treated cells (Fig. 1 *A–F*). The occurrence of TNF-induced cell death was monitored on the basis of the appearance of fluorescent nuclei (red) due to the uptake of PI. PI is a polar tracer that becomes fluorescent when it intercalates into DNA, but which, due to its polarity and ionic charge, is excluded from cells with an intact plasma membrane (23). Consequently, red fluorescent nuclei are only detected in cells with membrane damage. Untreated cells (Fig. 1 *A–C*) showed a weak but homogeneous accumulation of R123 due to ROIs produced by the basal oxidative metabolism. Under these conditions, no dead cells (red fluorescent nuclei) were observed. Cells treated with TNF for 4 hr (Fig. 1 *D–F*) showed a heterogeneous response: part of the cells exhibited an enhanced R123 fluorescence and, thus, an increased ROI formation; others showed fluorescent nuclei due to the uptake of PI, indicating cell death; and only few cells kept a normal appearance. Among the PI-stained (red) dead cells in Fig. 1 *D–F*, a single cell (arrow) showed enhanced R123 fluorescence (green), whereas the others had strongly reduced levels of fluorescence. Analysis of the sequence of TNF-induced ROI formation and cell death by repeated observation of identical fields revealed that increased R123 fluorescence and, thus, ROI production consistently preceded cell death. The latter was followed by a sharp drop of R123 fluorescence apparently as a consequence of plasma membrane disruption and subsequent loss of mitochondrial transmembrane potential. These observations allow us to conclude that (*i*) the TNF-mediated cytotoxic response evolves asynchronously in the cell population; (*ii*) TNF-induced ROI formation and cell death are closely correlated, the former preceding the latter; (*iii*) TNF-induced increment in R123 fluorescence intensity is generated by intracellular oxidation of the DHR123 probe, since cells with unaltered ROI levels remain present in proximity of enhanced radical-producing cells. The intracellular location of these ROIs was confirmed by the lack of interference by the membrane-impermeable ROI-scavenging enzymes catalase and superoxide dismutase with TNF-induced R123 fluorescence (data not shown).

TNF-Induced ROI Formation Is Causally Related to TNF-Mediated Cytotoxicity in L929 Cells. To further document the role of ROI formation in TNF-induced cytotoxicity, we followed the kinetics of both phenomena by flow cytometry, which allows the analysis of large cell populations. TNF-induced cell death was monitored on the basis of the reduced FALS properties of affected cells as described (18). Briefly, collapsed cells are detected as a distinct population exhibiting reduced FALS (Fig. 2 *Inset*, map 2). Cellular collapse has been shown to accompany loss of clonogenic potential and to correlate with irreversible membrane damage and, hence, represents cell death (18). The R123 fluorescence distribution was measured exclusively in the viable cell population (Fig. 2 *Inset*, map 1). Fig. 2 shows the increment of the mean DHR123-derived R123 fluorescence and of cell death in TNF-treated cultures relative to untreated cultures. After 2 hr and shortly before the first appearance of collapsed cells, a small but significant fraction of the population showed an increased R123 fluorescence intensity, causing a small increment of the mean R123 fluorescence. The mean fluorescence further increased as a function of time, since a larger fraction of cells produced higher ROI levels. This ROI response evolved in parallel with the progression of the cytotoxic response (Fig. 2), confirming the close correlation between both features as indicated by confocal microscopy.

To further investigate the nature of the relationship between TNF-induced ROIs and TNF-induced cytotoxicity, the ROI response was measured in two TNF-resistant L929 variants (16). In fully resistant L929r1 cells, TNF signal transduction is completely blocked because of the lack of TNF receptors. In

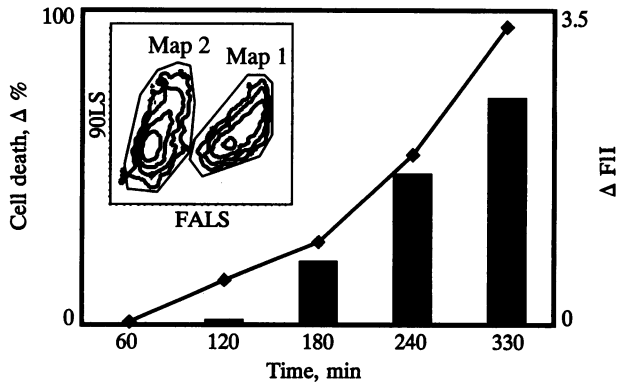

FIG. 2. Flow cytometric analyses of TNF-induced ROI production and cytotoxicity in L929 cells. Kinetics of TNF-induced ROIs (◆) and cell death (bars) as analyzed by flow cytometry. TNF-induced cell death represents the percentage of dead cells in TNF-treated cultures, measured as described in text, and corrected for spontaneous cell death in the untreated culture (0.5–1% throughout the experiment). ROI production was analyzed on the basis of TNF-induced DHR123 oxidation resulting in an increment of the mean R123 fluorescence intensity (ΔFII) expressed in arbitrary units. Mean ΔFII values were derived from single-parameter R123 fluorescence histograms from TNF-treated and TNF-untreated samples collected at the corresponding time points. The basal level of R123 fluorescence in untreated samples steadily increased during the experiment (from 3 at 60 min to 5.5 at 330 min). (*Inset*) Two-parameter contour maps of FALS and 90LS of L929 cells treated with TNF at 1000 IU/ml for 4 hr. Map 1 represents the viable cell population. Cells that collapsed as a result of TNF activity are contained in map 2 (18). The number of cells within both maps is used to derive the percentage of dead cells present in untreated and TNF-treated cultures.

L929r2 cells, the number and affinity of the TNF receptors are unaltered, but the cytotoxic activity of TNF is abrogated. However, in these cells, the TNF signal is still transduced, as demonstrated by the TNF-induced expression of the IL-6 gene. Furthermore, in the presence of CHX, an inhibitor of protein synthesis, L929r2 cells become sensitive to the cytotoxic activity of TNF. As expected, none of the TNF-induced parameters, such as IL-6 gene expression, cytotoxicity, or enhanced ROI production, could be observed in L929r1 cells (Table 1). Reduced TNF induced IL-6 gene expression, but neither ROI production nor cytotoxicity was observed in L929r2 cells. However, in the presence of the sensitizing drug CHX, L929r2 cells showed a cytotoxic response that was accompanied by ROI formation, similar to the events observed in the sensitive parental cells. Thus, a TNF-mediated ROI response is observed exclusively under conditions where TNF induces signal transduction resulting in cytotoxicity. This result strongly

Table 1. Comparison of TNF-induced IL-6 gene expression, cytotoxicity, and ROI production in L929 variants exhibiting different responsiveness to TNF

	TNF			TNF/CHX	
Cell line	IL-6	ROI	Cell death	ROI	Cell death
L929	360	0.8	60	2.0	90
L929r1	0	0	0.5	0	0.5
L929r2	135	0.01	0.2	0.8	43

Normalized amount of TNF-induced IL-6 bioactivity in culture supernatant, expressed as pg/ml from 4×10^5 cells after 5 hr of TNF treatment (1000 IU/ml). Background values in the absence of TNF were 10 pg/ml (L929), 60 pg/ml (L929r1), and 23 pg/ml (L929r2). ROI is expressed as the TNF-induced increment of DHR123-derived R123 fluorescence intensity after 6 hr of TNF treatment. Cell death is expressed as the percentage of TNF-induced, collapsed cells, detected by flow cytometry after 6 hr of TNF treatment. Data are from a representative assay.

suggests that the observed ROI production is part of the pathway leading to cytotoxicity.

To establish whether these radicals exert cytocidal activity, the scavenging of TNF-induced ROI by BHA or BHT was analyzed and compared to the capacity of these compounds to protect against TNF cytotoxicity. IL-6 was included in these experiments as a control on noncytolytic signaling (Fig. 3). When BHA was added at the same time as TNF, neither ROI induction (Fig. 3*A*) nor cell killing (Fig. 3*B*) occurred. Since the radical scavenger also interfered with early signal transduction, as indicated by decreased IL-6 gene induction, BHA was also added to the cell cultures 3 hr after TNF, this is at the start of the ROI response and after early signal transduction. As shown in Fig. 3*A*, this treatment did not alter the already existing level of R123 fluorescence, but completely blocked further increase in fluorescence and, hence, the production of free ROIs and additional cell death (Fig. 3*B*). BHT was less effective than BHA in scavenging the newly generated free radicals (Fig. 3*C*) and in protecting L929 cells against cytotoxicity (Fig. 3*D*). This lower activity of BHT correlates well with its lower efficiency as a radical scavenger measured in a similar cellular system by using exogenous H_2O_2 to generate oxidative stress within the cells (data not shown). The correlation between the capacity of both antioxidants to scavenge TNF-induced free radicals and to protect against TNF cytotoxicity strongly suggests that TNF-induced ROIs not only correlate with the cytotoxic response but also are directly cytocidal and/or represent an essential step in the pathway leading to cell death.

TNF-Induced ROIs Are Largely Scavenged by Mitochondrial GSH. Reduced GSH protects cells from oxidative damage by scavenging peroxides in the cytosol and in mitochondria and other organelles. In the mitochondria, the GSH redox system is the most important antioxidant defence, as there is no or very little catalase activity in the mitochondrial matrix (24). To determine whether GSH also scavenges ROIs generated by TNF, cells were treated with DEM, a drug that reacts with free sulfhydryl groups, resulting in a rapid depletion of

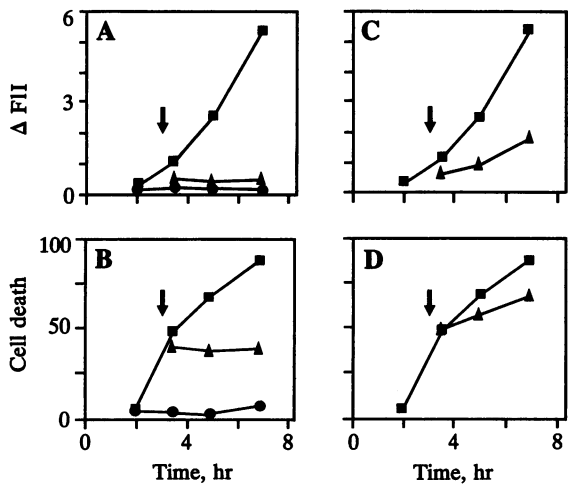

FIG. 3. Effect of the synthetic antioxidants BHA (*A* and *B*) and BHT (*C* and *D*) on TNF-induced ROI formation (*A–C*) and cell death (*B–D*) in L929 cells. DHR123-derived fluorescence intensity and cell death were analyzed simultaneously by flow cytometry as described in Fig. 2. Suspension cultures of L929 cells were treated with TNF at 1000 IU/ml. BHA or BHT at 50 μM was added at the same time as TNF (BHA) or 3 hr after TNF as indicated by the arrow (BHA and BHT). ΔFII indicates mean fluorescence intensity of TNF-treated cells minus the basal mean fluorescence intensity of untreated cells in the absence or presence of the respective antioxidants. ■, No antioxidant; ●, antioxidant at 0 hr; ▲, antioxidant at 3 hr. TNF-induced IL-6 production by 4×10^5 cells in the supernatant (after a 12-hr treatment) was 1460 pg/ml (no antioxidant), 60 pg/ml (BHA at 0 hr), and 586 pg/ml (BHA at 3 hr).

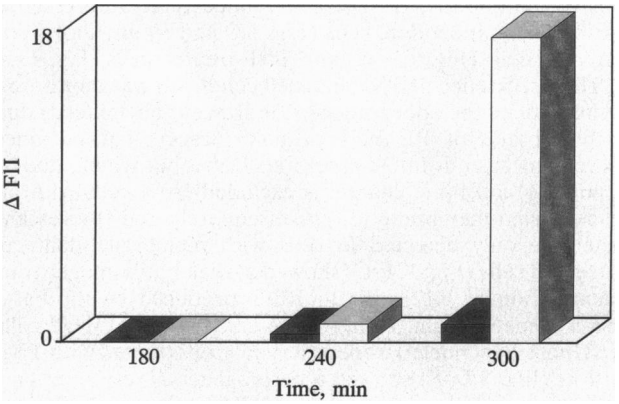

FIG. 4. Effect of blocking intracellular −SH groups by DEM on TNF-induced ROI production in L929 cells. Suspension cultures of L929 cells were stained with DHR123 and analyzed as described in Fig. 2. DEM (3 mM) was added to the cultures 3 hr after addition of TNF (1000 IU/ml) and DHR123. TNF-induced R123 fluorescence represents the mean fluorescence intensity of TNF-treated cells minus the basal mean fluorescence intensity of untreated cells in the absence (solid bars) or presence (open bars) of DEM.

GSH. Exposure of the cells to 3 mM DEM resulted within 30 min in a decrease in >90% of GSH content, as determined by staining with monochlorobimane (25). Addition of DEM and TNF simultaneously blocked all ligand-induced signaling, presumably because −SH-containing proteins are involved. Therefore, DEM was added 3 hr after TNF, i.e., when the phase of early signaling events is over and when TNF-generated ROIs become apparent. Under these conditions, a 20-fold increase in level of TNF-induced ROIs was observed (Fig. 4). The amplitude of this increment demonstrates that normally the majority of TNF-induced ROIs are scavenged by endogenous GSH.

Unlike the increment observed with DEM, the TNF-induced ROI response was not affected by pretreatment of the cells with BSO or BCNU (data not shown). These drugs decrease the cellular GSH content by blocking GSH synthesis and GSH reductase, respectively (24). In L929 cells, a 50% reduction of GSH was observed after a 24-hr treatment with BSO and up to 75% after a 7-hr treatment with BCNU. However, both inhibitors mainly deplete the cytosolic GSH content but do not affect appreciably the mitochondrial pool (26, 27). DEM, presumably depletes both the cytosolic and mitochondrial GSH pools, as supported by the nearly complete loss of GSH in treated cells. Hence, the differential effects of DEM vs. BSO and BCNU suggest that mitochondrial GSH, and not cytoplasmic GSH, acts as the major endogenous scavenger of the TNF-induced ROIs.

DISCUSSION

Multiple cellular pathways leading to cell death have been described, including perturbation of ion homeostasis (28), activation of proteases and phospholipases, degradation of DNA, and ROI generation. Despite a vast number of studies on the mechanism of TNF-induced cell death, the molecular basis of its cytotoxic action is still not fully understood. We showed previously that murine L929 fibrosarcoma cells are killed by TNF via a necrotic process, characterized by swelling of the cytoplasm followed by permeabilization and lysis of the plasma membrane accompanied by cellular collapse (18). Furthermore, we have documented that mitochondria play a crucial role in causing TNF-induced cytotoxicity in TNF-sensitive L929 cells (12, 13). These results were indicative of an involvement of mitochondrial production of ROIs in the TNF-signaling pathway. However, the actual formation of

these ROIs or their mechanism(s) of action has not yet been demonstrated directly.

The present study provides qualitative and quantitative data on the induction of ROI formation in mitochondria upon TNF stimulation in L929 cells. The production of intracellular ROIs was analyzed by using the fluorogenic marker DHR123 in combination with CLSM and flow cytometry. Both methods revealed a significant increase of intracellular ROI formation in TNF-treated cells. This increase preceded plasma membrane permeabilization, suggesting a link between both events. Cell killing by other toxic agents, such as CHX, a protein synthesis inhibitor, and myxothiazol, an inhibitor of mitochondrial complex III, did not lead to increased DHR123 oxidation, indicating that the observed formation of ROIs is not a general feature of cell death.

L929r2 cells exhibit resistance to the cytotoxic effect of TNF (16). Only in the presence of CHX did TNF stimulation of these cells lead to ROI formation, and under these conditions the cells became susceptible to the cytotoxic action of TNF. These L929r2 cells still showed inducible, albeit reduced, expression of IL-6, but the threshold level of inducible ROIs may be much lower for the activation of the NF-κB transcription factor than for cytotoxicity.

Several reports have implicated ROI formation in the TNF-mediated cytotoxic process on the basis of the protective effect exerted by synthetic or naturally occurring radical scavengers (4, 5, 12). However, not all radical scavengers are equally protective, thus raising doubts on the exact mechanism by which these compounds inhibit cytotoxicity. Here we show that the protective activity of the synthetic radical scavengers BHA and BHT against the cytotoxic activity of TNF directly correlates with their capacity to scavenge oxygen radicals generated by TNF. BHA was more effective in scavenging the TNF-induced ROIs than BHT and was more efficient in protecting cells against TNF cytotoxicity. The radical scavengers added at the same time as TNF blocked the cytocidal activity of TNF and drastically decreased the IL-6 gene induction, probably by a much decreased activation of transcription factors. However, when the radical scavengers were added 3 hr after TNF, further ROI production and cytocidal activity were completely blocked, while IL-6 gene expression was only slightly inhibited.

The question remains as to why and how the relatively small increment of free radicals contributes to cell death. A possible explanation may be derived from our observation that depletion of the cytosolic and mitochondrial GSH pools, but not depletion of the cytosolic pool, causes a major increase in TNF-induced free radicals. Apparently, 80–95% of ROIs formed are normally scavenged by the mitochondrial GSH redox system. This scavenging by GSH may cause an imbalance in the thiol status and, hereby, affect the Ca^{2+} homeostasis in the mitochondria. These phenomena have been reported to be involved in oxidative-stress-related cell death (26, 28) and, thus, may contribute to the cytocidal activity of TNF-induced ROIs by rendering mitochondria more vulnerable to oxidative attack. Alternatively, excess free ROIs may cause peroxidation of lipids of the plasma membrane, leading to membrane permeabilization and cell death. The latter mechanism is indirectly supported by our observation that mitochondria of permeabilized cells still retain R123 for a short period and thus are functional at the time the cells are irreversibly damaged. Experiments to elucidate the exact mechanism of a perturbed mitochondrial electron flow as a direct cause of ROI production and to identify the mediator that transmits the cytosolic TNF signal to the mitochondria, should contribute to the further understanding of the molecular mechanism underlying TNF-induced cytotoxicity.

We acknowledge Dr. H. Raes and Mr. J. Vanderheyden for technical facilities. This research was supported by the Interuniversitaire Attractiepolen, the Fonds voor Geneeskundig Wetenschappelijk Onderzoek, the National Lottery, and a European Community Biotech Program. V.G. and K.D.V. thank the Vlaams Instituut voor de Bevordering van het Wetenschappelijk-technologisch Onderzoek in de Industrie for a fellowship.

1. Fiers, W. (1995) in *Biologic Therapy of Cancer*, eds. DeVita, V. T., Jr., Hellman, S. & Rosenberg, S. A. (Lippincott, Philadelphia), 2nd Ed., pp. 295–327.
2. Beyaert, R. & Fiers, W. (1994) *FEBS Lett.* **340,** 9–16.
3. Suffys, P., Beyaert, R., Van Roy, F. & Fiers, W. (1987) *Biochem. Biophys. Res. Commun.* **149,** 735–743.
4. Matthews, N., Neale, M. L., Jackson, S. K. & Stark, J. M. (1987) *Immunology* **62,** 153–155.
5. Zimmerman, R. J., Chan, A. & Leadon, S. A. (1989) *Cancer Res.* **49,** 1644–1648.
6. Wong, G. H. W. & Goeddel, D. V. (1988) *Science* **241,** 941–944.
7. Van Lint, J., Agostinis, P., Vandevoorde, V., Haegeman, G., Fiers, W., Merlevede, W. & Vandenheede, J. R. (1992) *J. Biol. Chem.* **267,** 25916–25921.
8. Vietor, I., Schwenger, P., Li, W., Schlessinger, J. & Vilček, J. (1993) *J. Biol. Chem.* **268,** 18994–18999.
9. Wiegmann, K., Schütze, S., Machleidt, T., Witte, D. & Krönke, M. (1994) *Cell* **78,** 1005–1015.
10. Halliwell, B. & Gutteridge, J. M. C. (1990) *Free Radicals in Biology and Medicine* (Clarendon, Oxford).
11. Schreck, R., Rieber, P. & Baeuerle, P. A. (1991) *EMBO J.* **10,** 2247–2258.
12. Schulze-Osthoff, K., Bakker, A. C., Vanhaesebroeck, B., Beyaert, R., Jacob, W. A. & Fiers, W. (1992) *J. Biol. Chem.* **267,** 5317–5323.
13. Schulze-Osthoff, K., Beyaert, R., Vandevoorde, V., Haegeman, G. & Fiers, W. (1993) *EMBO J.* **12,** 3095–3104.
14. Emmendörffer, A., Hecht, M., Lohmann-Matthes, M.-L. & Roesler, J. (1990) *J. Immunol. Methods* **131,** 269–275.
15. Rothe, G., Emmendörffer, A., Oser, A., Roesler, J. & Valet, G. (1991) *J. Immunol. Methods* **138,** 133–135.
16. Vanhaesebroeck, B., Van Bladel, S., Lenaerts, A., Suffys, P., Beyaert, R., Lucas, R., Van Roy, F. & Fiers, W. (1991) *Cancer Res.* **51,** 2469–2477.
17. Russell, W. C., Newman, C. & Williamson, D. H. (1975) *Nature (London)* **253,** 461–462.
18. Grooten, J., Goossens, V., Vanhaesebroeck, B. & Fiers, W. (1993) *Cytokine* **5,** 546–555.
19. Fransen, L., Müller, R., Marmenout, A., Tavernier, J., Van der Heyden, J., Kawashima, E., Chollet, A., Tizard, R., Van Heuverswyn, H., Van Vliet, A., Ruysschaert, M. R. & Fiers, W. (1985) *Nucleic Acids Res.* **13,** 4417–4429.
20. Ostrove, J. & Gifford, G. (1979) *Proc. Soc. Exp. Biol. Med.* **160,** 354–358.
21. Van Snick, J., Cayphas, S., Vink, A., Uyttenhove, C., Coulie, P. G., Rubira, M. R. & Simpson, R. J. (1986) *Proc. Natl. Acad. Sci. USA* **83,** 9679–9683.
22. Griffith, O. W. & Meister, A. (1985) *Proc. Natl. Acad. Sci. USA* **82,** 4668–4672.
23. Tanke, H. J., van der Linden, P. W. & Langerak, J. (1982) *J. Immunol. Methods* **52,** 91–96.
24. Reed, D. J. (1990) *Annu. Rev. Pharmacol. Toxicol.* **30,** 603–631.
25. Shrieve, D. C., Bump, E. A. & Rice, G. C. (1988) *J. Biol. Chem.* **263,** 14107–14114.
26. Casini, A. F., Pompelia, A. & Comporti, M. (1985) *Am. J. Pathol.* **118,** 225–237.
27. Griffith, O. W. & Meister, A. (1985) *Proc. Natl. Acad. Sci. USA* **82,** 4668–4672.
28. Richter, C. (1993) *FEBS Lett.* **325,** 104–107.